Catalyst Research Volume 23, Issue 2, October 2023 Pp. 2226-2244

FLOOD HAZARD ASSESSMENT AND MAPPING USING GIS AND POTENTIAL RISK REGION USING THE AHP MODEL: A CASE STUDY OF NARUDAIYAR WATERSHED, TAMIL NADU, INDIA.

Anbudhasan.D[1]*, K. Ezhisaivallabi [2]

[1*]Research Scholar, Department of Civil Engineering, Annamalai University, Chidambaram, Tamil Nadu, India.

[2] Associate Professor, Department of Civil Engineering, Annamalai University, Chidambaram, Tamil Nadu, India.

Corresponding Author Email; danbudhasan@gmail.com

Abstract

Flooding is one of the most widespread catastrophes caused by nature which impacts literally every region of the environment, with one notable exception of the polar areas. Floods are a common natural calamity that has a significantly negative impact on people and environmental resources, particularly in the Narudaiyar Watershed. The principal objective of the current research is to pinpoint flood-prone segments along the Narudaiyar Watershed using satellite imagery and GIS (Geographic Information System) data, in addition to applying the Multi-criteria Decision-Making-Analysis (MCDM) Analytical Hierarchy Process (AHP) simulation in cartographic circumstances. Weights for flood-causing components have been calculated from the AHP approach using a (10*10) decision matrix, indicating their different priorities ranging from extreme to low priority, such as proximity to river (13.25%), Topographic Wetness Index (TWI) (13.58%), precipitation (13.25%), gradient (9.84%), the kind of soil and density of outflow (9.23%), Land use Landover (LULC) (6.59%), Normalized vegetative index (NDVI) (5.63%), and proximity to road (5.73%). Also, it was discovered that roughly 37% of the entire area of 1844 km2 had a high likelihood of flooding; in order to lower the danger, local and national authorities must pay special attention to these areas. The outcomes of this research will be an essential resource for legislators in determining appropriate mitigation strategies in regions susceptible to flooding zones.

Keywords: Flood Susceptible zone, AHP, ArcGIS, MCDM, and Vulnerable zones.

Introduction

Flooding is a phenomenon of nature that generates short-term land submersion as a result of significant rainfall periods that occur swiftly. Flooding refers to the circumstance of partially or completely submerging typically dry areas as a result of runoff that has accumulated quickly (Jeb & Agarwal 2008). Flooding is the most widespread catastrophe caused by nature in the world, causing significant hazards to humanity's lives, possessions, and way of existence. It also has the potential to hasten soil erosion. Since floods are a very complicated phenomenon, experts from all over the world have always been drawn to study them and try to figure out how to manage and prevent them better. There are a number of both natural and human elements that can cause a calamitous flood incident. According to the latest research, environmental change has a significant role in fatal drownings. The results of these studies (Rojas et al., 2012) proved that climate change

Catalyst Research Volume 23, Issue 2, October 2023 Pp. 2226-2244

might modify land use patterns and generate an inaccessible terrain, which may contribute to stream acceleration in addition to atmospheric conditions (Khosravi et al., 2016). Using a combination of geographic information systems, remote sensing, and multi-criteria decision analysis, flood-inundated areas have been mapped the flood hazard zones (Fernandez et.al., 2016). There are estimates that within the previous two centuries, floods have had an impact on around 1.5 billion people worldwide (Khole et al.,2013). Extreme rainfall that has been observed in recent decades is a direct result of climate change. Climate model simulations and actual data both show that rising temperatures brought on by more water vapor cause more instances of precipitation events, which raises the danger of flooding (Hennessey et al.1997). According to the Inter-governmental Panel on Climate Change (IPCC 2007), wet extremes will likely increase in the future, although the average amount of precipitation will be increasing. Although significant precipitation has occurred lately in many different parts of India, the effects of significant precipitation events may be helpful when it comes to flood management. Recent examples include incidents that took place in 2014 and 2015 as a result of multi-day cloud bursts concentrated in the states of Uttarakhand and Jammu & Kashmir, respectively. According to several studies regarding catastrophic rainfall events, the magnitude of such events in India's central areas could increase in the future. Tamil Nadu is one of India's most maritime-vulnerable states in this regard because of its geographic location, making it especially susceptible to tropical cyclones and the storm surges that go along with them. Moreover, it frequently experiences extreme weather, such as floods in coastal zones (Bal et al.2015). Flood Hazard maps provide valuable and vital information to help individuals and authorities understand the potential risks of natural catastrophes, as well as to aid in emergency preparedness and management. As a result of these factors, numerous professionals all through the world have competently distinguished potential flooding zones utilizing GIS-AHP techniques (Ouma & Tateishi 2014).

Study Area

The Research area has been constrained to a river of a major carrier branch of Cauvery and it splits from the Cauvery at the Upper Anicut in Tiruchirappalli District. It travels to a distance of 100 miles through Trichy, Perambalur, Ariyalur, Thanjavur, Mayiladuthurai, Cuddalore District, and emptied into the Bay of Bengal. According to the Cauvery Water Dispute Tribunal, Lower Anaicut is the ultimate barrage for offering river water across the Cauvery River system. As illustrated in Figure 1, 10 tmcft of water is allotted for the limited environmental flows downstream of the lower Anicut. The study area covers a geographical area of 1844 km2, and its longitude and latitude extend from 79o08’’08E to 79o 50”01E and 10o59” 27N to 11o 27” 05 N. Extreme weather events like flooding frequently affect it, especially in coastal areas. The intensity of rain is greater along the coastal length during the minimal pressure formed in the Bay of Bengal, with the average rainfall in coastal regions ranging from (970 to 1500 mm). Almost all of this region experiences severe flooding during the north eastern monsoon. Additionally, it has a comfortable tropical climate year-round, with summer temperatures averaging between 22 and 36 °C and winter temperatures ranging between 21 and 33°C.

Catalyst Research Volume 23, Issue 2, October 2023 Pp. 2226-2244

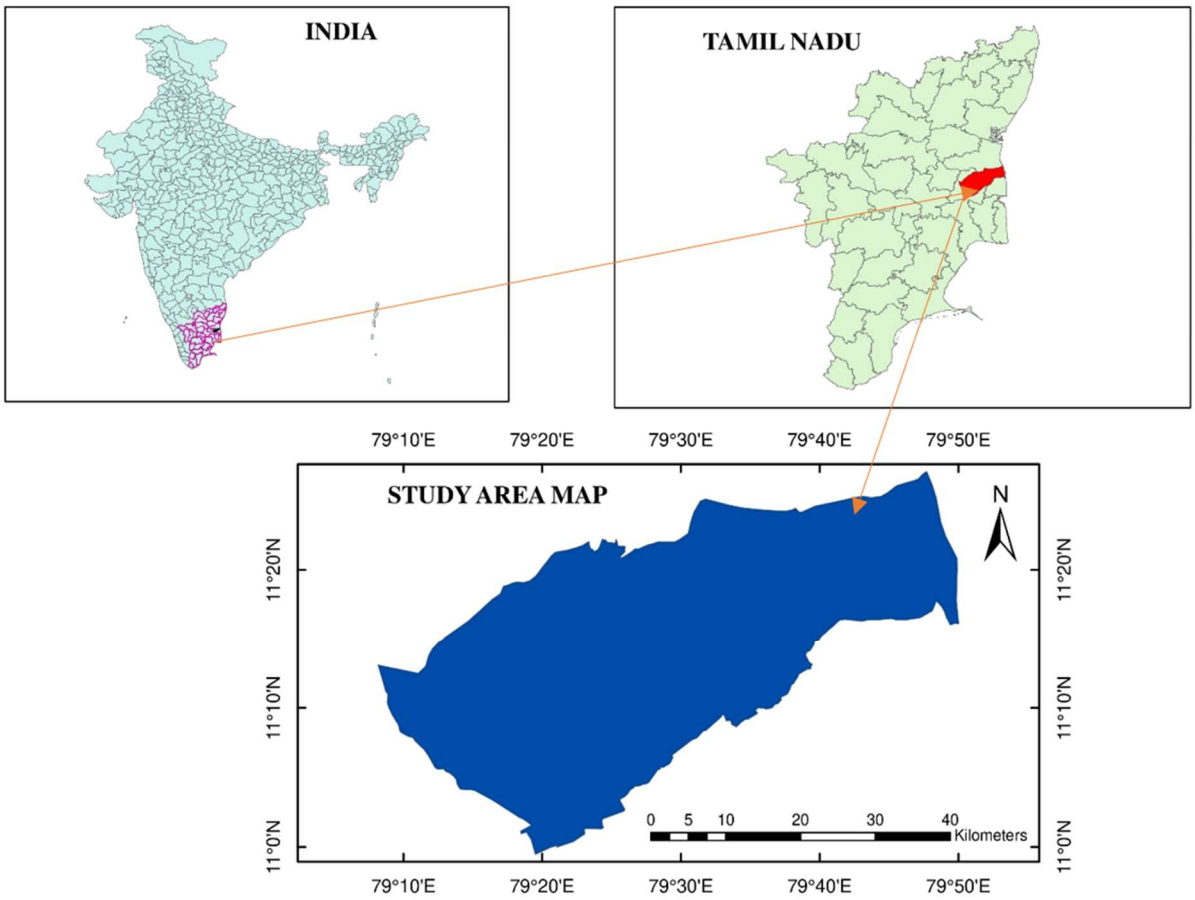

Figure 1. Study area map of Narudaiyar Watershed

Materials and Methods

The study concentrated on flood hazard assessment in the Narudaiyar Watershed, and multiple datasets with sequential steps of techniques were used. The current research employed ArcGIS 10.8.1 to generate an Analytical hierarchy process (AHP) model in tandem with earth observation and geographic data management systems for cartographic achievement. The ten factors of flood-influencing physical variables, including DEM, gradient, TWI, precipitation, the density of outflow, LULC, NDVI, kind of soil, proximity to the river, and proximity to the road, are needed for the model's formulation (Ali et al. 2019). Table (1a) provides a description of the datasets used in this research. A flood hazard zone map has been generated based on this data to highlight spots with extremely high, high, moderate, minimal, and extremely low flood susceptibility. The flood Risk map was validated using a flood deluge map generated from Sentinel 1A satellite photos.

Table (1) Sets of information used in the study

S. no	Quantities	Commodities	Dimensions	Obtain
1	Digital Elevation Model (DEM)	SRTM (DEM)	Thirty m	USGS earth explorer https://earth explorer.usgs .gov/ USGS earth explorer
2	LANDSAT-8	Downloadable	Thirty m	https ://earth explrer.usgs .gov/

Catalyst Research Volume 23, Issue 2, October 2023 Pp. 2226-2244

3	Soil	Digitized from soil texture map	-	FAO Soil Data Base on Worldwide.(https://www.fao.org/)
4	Rainfall	Ariyalur, Thanjavur, Mayiladuthurai, Cuddalore District Using (IDW) analyst tool	mm	Indian Meteorological Department (IMD) https://www.imdpune.gov.in/ & Institute of water studies (IWS), Tamilnadu,Chennai.
5	Slope	Derived from DEM	m	USGS earth explorer https ://earth explorer.usgs .gov/
6	NDVI	LANDSAT-8	m	USGS earth explorer https ://earth explorer.usgs .gov/
7	Topographic Wetness Index (TWI)	SRTM (DEM)	m	USGS Earth Explorer https ://earth explorer.usgs .gov/
8	Distance From River	Derived From DEM	m	USGS earth explorer https ://earth explorer.usgs .gov/
9	Density of outflow	Derived from DEM	30 m	USGS Earth Explorer https ://earth explorer.usgs .gov/
10	Distance From Road	Derived from (OSM)	-	(OSM) Data https ://openstreetmap.org

Methods

In this research, the flood vulnerable zone was established in a number of stages, including recognizing and defining the complex problem, establishing an AHP model-based organizational framework for the selected criteria, performing a two-way via a matrix technique for the specified shaping components (binary comparison), evaluating priorities and establishing proportional weights for each variable, measuring uniformity value for the evaluations, and addressing outcomes. In order to calculate the likelihood that certain elements may be included in the flood hazard, the weighting of ten specified flood initiation variables was analyzed using an AHP model constructed on the MCDM. To obtain appropriate weights, the previously indicated contributing variables were then separated into sub-classes (Danumah et al. 2016).

Catalyst Research Volume 23, Issue 2, October 2023 Pp. 2226-2244

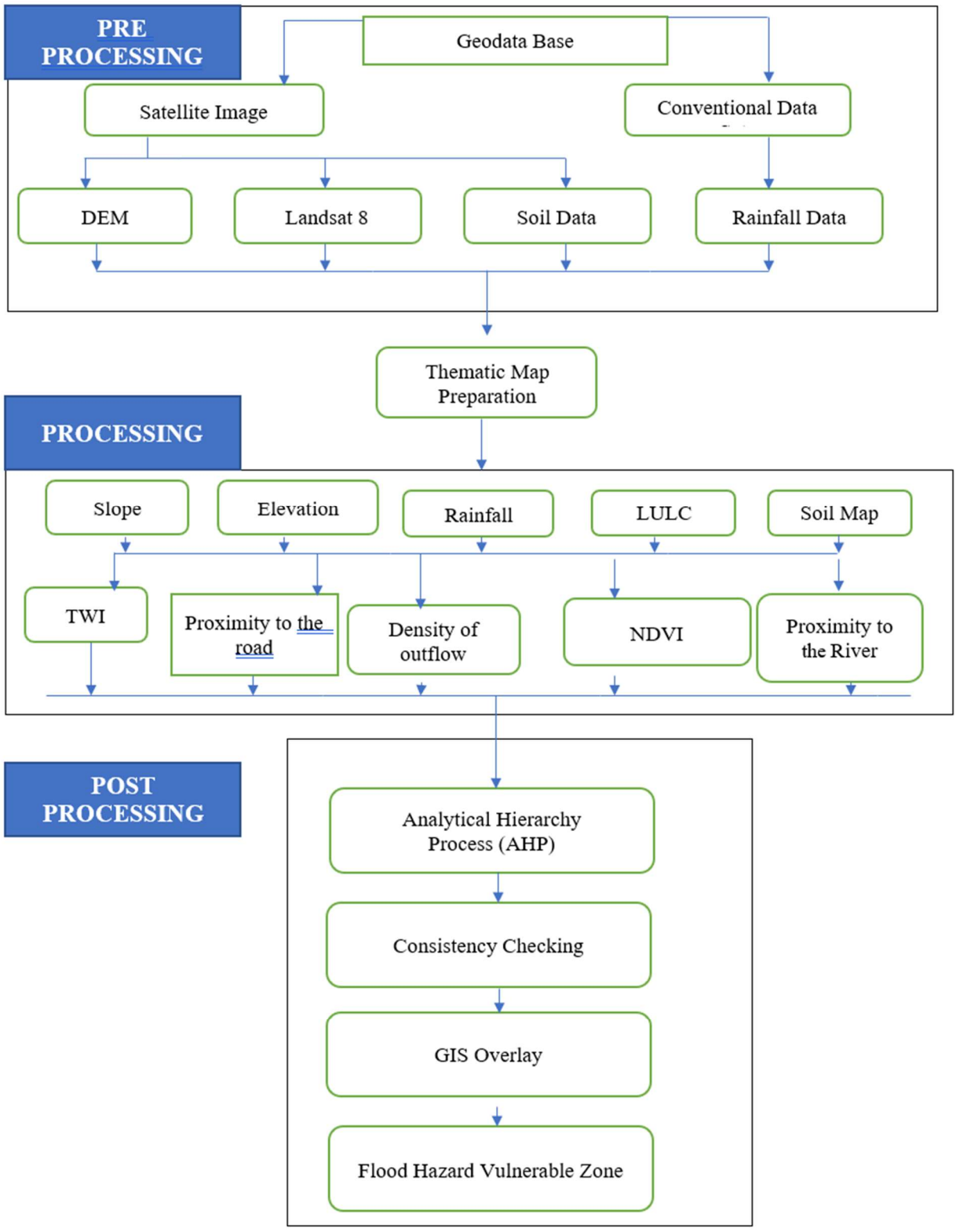

Figure 2. Flow Chart of Methodology

Catalyst Research Volume 23, Issue 2, October 2023 Pp. 2226-2244

Analytical Hierarchy Process (AHP) model

AHP had originally been employed in decision-making involving multiple criteria by (Saaty 1980; Dou et al.,). The AHP is a tool for supporting decisions. It employs a multi-level hierarchical framework of goals, standards, sub-standards, and options to address complicated decision-making problems. For the flood-vulnerable zones (FVZ), it establishes the weights and rankings of several parameters. All of the theme layers have been prepared using the AHP model. By categorizing the data-derived thematic maps into five vulnerability categories, an AHP-based juxtaposition matrix of the various variables mentioned supra is generated. (Table 6). The model is used to compare each of the ten distinct elements with parameter weights, and each of the ten variables was scored on an established scale from 1 to 9 (Table 1) based on their relative significance (Saaty 1980).

Table 1 Pair-wise comparison scale weights on the basis of the AHP scale (Saaty 1980)

Grade on the basis of integers	Choice Judgments rendered vocally
1	The instances are advised
2	Likewise to slightly
3	Frequently endorsed
4	Mildly to passionately
5	Most likely beneficial
6	Fervently to diverge forcefully
7	Incredibly voiced
8	Exceedingly decisively to incredibly significantly
9	Firmly favored

By splitting the total of every matrix element's columns, one can determine the size values, which vary from smaller to larger. However, the row averages are calculated in order to derive the priority vector.

Table 2 Correlation of 10 X 10 preference matrix couples

Parameters	Twi	Elevation	Gradient	Precipitation	Land use	NDVI	Proximity to the river	Proximity to the Road	Density of outflow	Kind of Soil
Twi	1	1	1	1	3	5	1	3	1	1
Elevation	1	1	1	1	2	5	2	2	1	1
Gradient	1	1	1	1	3	1	1/2	1	1	1
Precipitation	1	1	1	1	3	2	2	3	1	1
Land use	1/3	1/2	1/3	1/3	1	1	1/3	3	1	1
NDVI	1/5	1/5	1	1/2	1	1	1/5	1	1	1
Proximity to river	1	1/2	2	1/2	3	5	1	3	1	1
Proximity to road	1/3	1/2	1	1/3	1/3	1	1/3	1	1	1
Density of outflow	1	1	1	1	1	1	1	1	1	1
Kind of soil	1	1	1	1	1	1	1	1	1	1
sum	**7.87**	**7.70**	**11/3**	**7.67**	**18.33**	**23.00**	**9.37**	**19.00**	**10.00**	**10.00**

Catalyst Research Volume 23, Issue 2, October 2023 Pp. 2226-2244

Consistency ratio

To smooth up the newly formed pair-wise matrix and its stated weightage mechanism, use the subsequent algorithm (Saaty 1980). The ratio of consistency (CR) was established for evaluation, with an acceptable CR being less than 0.1. The uniformity of the accomplished Eigenvector-matrix gathered in the current research is 0.093, demonstrating that the set of decisions n evaluated as satisfactory.

$$CR = \frac{CI}{RI} \quad \text{Eq.1}$$

CI is computed using Eq.2

$$CI = \frac{\lambda max - n}{n-1} \quad \text{Eq.2}$$

Where CR stands for consistency ratio, CI stands for consistency index, and RI stands for random index. The absolute maximum Eigenvalue of the comparison matrix is expressed by maximum, whereas the total number of components or elements in a matrix is denoted by n. The homogeneity of the impulsively generated pair-wise lattice displayed in (Table 3) has been designated as RI. The data in the table have been presented to various AHP configurations. As a result, the established RI found in the study is 1.49 based on the 10 factors.

Table 3 Random Index (RI) value

Size of Matrix (n)	1	2	3	4	5	6	7	8	9	10
Random Index (RI)	0	0	1/28	0.9	1.12	1.24	1.32	1.41	1.45	1.49

$$FVI = \sum_{i=1}^{n} Wi * Ri \quad \text{Equation.3}$$

Where WI is the individual weight for each parameter's individual flood conditioning, and RI is the rating class. Finally, using natural breaks, the resulting Flood Vulnerable Zone was classified into five classes: extremely low, low, moderate, moderately high, and exceptionally high.

Results and Discussion

Slope

Because the gradient regulates the flow of surface water, a slit is an essential topographic feature for hydrological study (Tehrany et al. 2013, Mojaddadi et al. 2017, Das et al. 2018). The slope of the ground surface plays a crucial role in floods. The flood severity increases as the gradient throws and decreases as the slope ascents. According to Das and Pardeshi (2018), a region's channel slope and flow velocity are directly correlated. According to Masoudian (2009), as the river slope rises, so too does the river's flow velocity. The slope and infiltration are directly related. In areas with a lower surface slope, a large amount of water gets stagnant and creates a flood situation because an increase in slope slows the infiltration rate but increases surface runoff. The slope map was produced using a 30 m digital elevation model (DEM) from the Shuttle Radar Topographic Mission (SRTM) of the research, where the area runs from (0o to 57o) Figure 3.

Elevation (DEM)

Catalyst Research Volume 23, Issue 2, October 2023 Pp. 2226-2244

In flood hazard mapping studies, elevation is the most important component for controlling flood susceptibility (Botzen et al. 2012). Higher-elevation elevation places are often less susceptible to floods, but lower-elevation regions are more vulnerable. Because water flows down from higher vantage points, low-altitude locations with flat surfaces are more susceptible to flood (Das et al. 2018). Figure 4 shows the elevation range of the research area (0 to 119m).

Table 4 Formalized and Reinforced Pair-Wise Evaluation Matrix.

Class	Twi	Elevation	Gradient	Precipitation	Land use	NDVI	Proximity to the river	Proximity to the	Density of outflow	Kind of Soil	Weight	Weight in Percentage (%)
TWI	0.13	0.13	0.10	0.13	0.16	0.22	0.11	0.16	0.10	0.10	0.1358	13.58
Elevation	0.13	0.13	0.10	0.13	0.11	0.22	0.21	0.11	0.10	0.10	0.1367	13.67
Slope	0.13	0.13	0.10	0.13	0.16	0.04	0.05	0.05	0.10	0.10	0.0983	9.84
Precipitation	0.13	0.13	0.10	0.13	0.16	0.09	1/51	0.16	0.10	0.10	0.13249	13.25
LULC	0.04	0.06	0.03	0.04	0.05	0.04	0.04	0.16	0.10	0.10	0.0658	6.59
NDVI	0.03	0.03	0.10	0.07	0.05	0.04	0.02	0.05	0.10	0.10	0.0562	5.63
Proximity to the river	0.13	0.06	0.19	0.07	0.16	0.22	0.11	0.16	0.10	0.10	0.1325	13.25
Proximity to the river	0.04	0.06	0.10	0.04	0.02	0.04	0.04	0.05	0.10	0.10	0.0572	5.73
Proximity to the river	0.13	0.13	0.10	0.13	0.05	0.04	0.11	0.05	0.10	0.10	0.0923	9.23
Proximity to the river	0.13	0.13	0.10	0.13	0.05	0.04	0.11	0.05	0.10	0.10	0.0923	9.23

LAND USE AND LAND COVER

The main factors influencing how a particular area's landscape changes in land use and cover. Land use/Land cover map has been derived from Landsat-8 using classification under supervision and it is classified into eleven classes, which are then reclassified into six classes based on weights, such as class one Agricultural Land with an area of 1491/557 km2, second class Barren land with an area of 129.646 km2, third class urban area/built-up area with an area of 16.097 km2, fourth class River with an area rea of 138.823 km2, fifth class water bodies with an area According to the research, classes second and first are least susceptible to floods, nevertheless, classes third, fourth, fifth, and sixth are deemed highly susceptible.

Normalized Difference vegetation index (NDVI)

Another element that can be used to evaluate vegetation covering and how floods would affect a study area is the NDVI. NDVI assessments usually fluctuate between -1 and +1 in value. The

Catalyst Research Volume 23, Issue 2, October 2023 Pp. 2226-2244

following equation is used to determine the NDVI values for the map that was created using a LANDSAT 8 OLI satellite image:

$$NDVI = (NIR- VIS) / (NIR + VIS) \quad \text{Eq. 4}$$

The NDVI outcomes in the research area ranged from - 0.24 to 0.92 stating that the positive values reflect flora while the negative values show water. As a result, NDVI has an inverse association with flooding: greater NDVI levels suggest a reduced possibility of flooding, whereas lower NDVI values indicate a higher likelihood of flooding. The NDVI in this study ranged from -1/54 to 0.92, and it was divided into five distinct categories using the conventional brakes approach (see Figure 7).

Soil Type

Two key elements, such as soil type and texture, affect an area's ability to hold water and its characteristics for surface infiltration (Nyarko, 2002). The study region was split up into 8 different soil classes. The infiltration capacity was used to categorize the final map, and each soil type was given a certain amount of weight. The Coleroon River has clay loam, clay, loam and sandy loam, whereas the remaining research area is made up of different types of soil (see figure. 5).

Table 5 Different Soil Types in the Study Area.

S.No.	Soil type	Area in_km^2	Percentage of Soil Area
1.	Clay	24	1.30
2.	Clay Loam	418	22.66
3.	Sandy Loam	268	14.53
4.	Loam	1134	61.49
Total		1844	100 %

Proximity to River

One of the key elements in mapping overflow hazards is proximity to the river. The elevation and slope rise as the distance does as well. Furthermore, the Stream is usually the lowest point in that particular location. As a result, locations in further proximity to the river are less susceptible to flooding. During floods, river banks overflow, drowning the surrounding land that is dry. In this research, the proximity to the river has been divided into five class in Figure 9: very high (0-528 m), high (528-1,057 m), moderate (1,057-1,588 m), low (1,588-2,115 m), and very low (2,115-2644 m). Whatever it is to the river, the greater the likelihood it is to flood, and the more distant it is from the river, the less likely it is to flood.

Proximity to Road

The Proximity to the Road is a crucial consideration when calculating overflow vulnerability. Flood water reaches roads and streams during floods when water pours over riverbanks and into low-lying areas, damaging public property as well as homes, roads, and streams. The study divides the distance from the road assigned to 5 categories: Figure 10 shows values for exceptionally high (0-528 m), higher (528-1,057 m), moderate (1,057-1,588 m), lower (1,588-2,115 m), and

Catalyst Research Volume 23, Issue 2, October 2023 Pp. 2226-2244

extremely low (2,115-2644 m). Flood susceptibility increases with decreasing proximity to the River to the Road and drops as one rises in proximity of the river to the road.

Rainfall

The most notable aspect of this is that, although the coastal regions receive sufficient precipitation from both the northeast and southwest monsoons, the northeast monsoon season (October to December) is regarded as being rainier than the southwest monsoon. The Inverse Distance Weighted (IDW) Spatial Interpolation analyst tool in the software ArcGIS 10.8.1 has been used to produce the precipitation for the mean rainfall distribution map. This tool uses precipitation data from all rain gauge stations. For the years 31 between 1991 and 2022, the data is annual rainfall. Indian Meteorological Department (IMD) data on rainfall was gathered. As illustrated in (Figure 8), and are divided into five classes.

Topographical Wetness Index (TWI)

According to Gokceoglu et al. (2005), the topographic wetness index (TWI) shows how the topography affects runoff development and quantifies the flow accumulation at any place in stream catchments. The following is the formula for calculating the TWI:

$$TWI = \ln\left(\frac{As}{\tan Q}\right) \qquad \text{Eq. 5}$$

Whereas is the area in square meters per person, and Q denotes the degree of the local slope gradient. Flooding is more inclined to emphasize with an elevated TWI. In contrast, there is less vulnerability potential in the lower TWI zones. The computation of the TWI was made using SRTM DEM, and the TWI for the research region ranged from -7.77 to 12.9 m2. (see Figure 11).

Drainage Density (DD)

The density of drainage has an immediate impact on flood vulnerability. Hydrological tool and The ArcGIS line density tool is used to construct the density of the outflow map from the SRTM DEM. (30). The Whole research area is divided into five divisions: extremely low (0 to 1.17 km/km2), low (1.17 to 2.02 km/km2), moderate (2.02 to 3.95 km/km2), high (3.95 to 4.10 km/km2), and very high (4.10 to 6.22 km/km2). In a GIS, drainage density may be utilized alongside additional characteristics to assess which areas are most prone to floods. For gathering drainage network information, toposheets can be utilized; however, DEM-based elevation data has been generated and is more accurate (Forte and Strobl 2006) (see Figure 12).

Assessment of Flood Vulnerable Zone

Using ArcGIS 10.8.1's natural breaking method, the final flood susceptibility map shows values between 146 and 384 that are divided into five separate classes (Figure 13). The AHP tool which able to identify the zone of flooded area with the help of different of thematic layers weightage and its determine the zone of flooded area by using weighted sum overlay method. Class sizes are very small. 19%, 13%, 14%, 16%, and 37% respectively correspond to low, moderate, high, and extremely high flood probabilities. Chidambaram, which is flanked by the rivers Cuddalore and Kollidam, had the most severe risk of flooding due to the area's low height and slope. This region is particularly susceptible to natural disasters, notably catastrophes during the northeast monsoon (October to December), which is the most probable period for floods in this region. A moderate

Catalyst Research Volume 23, Issue 2, October 2023 Pp. 2226-2244

level of flood susceptibility is present in and around 28% of research region. The northeastern portion of the research area near the shore has a lower height and slope, making it more prone to water buildup which makes it more vulnerable to flooding. These locations are primarily agricultural along the coastal rivers and water bodies, and these areas are very high, high, and moderately affected. A moderate level of flood susceptibility is present in around 16% of the studied region. These areas are mostly agricultural near river mouths and wetlands, which are brutally, deeply, and moderately wrecked. Planners from across the globe have recently highlighted the importance of adopting GIS tools for decision-making in flood-prone areas since they save time and money. The supplied weights affect the AHP technique's accuracy. But the key finding is that different researchers' weighting and ranking of various parameters in their investigations varied unequally. The attempt to create a precise flood-vulnerable map depends on the precision, accessibility, and regional circumstances of the data in several criteria. By using AHP tool techniques which will save the duration to identify the suspectable zonal area of flooded and its easy to adopt the conservation structures whichever predicted zone of flooded area.

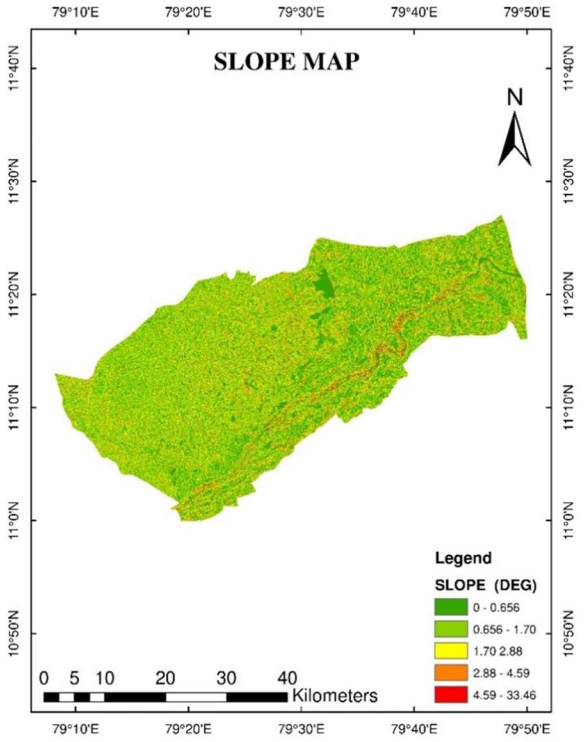

Figure 3 Slope Map of the Narudaiyar Watershed

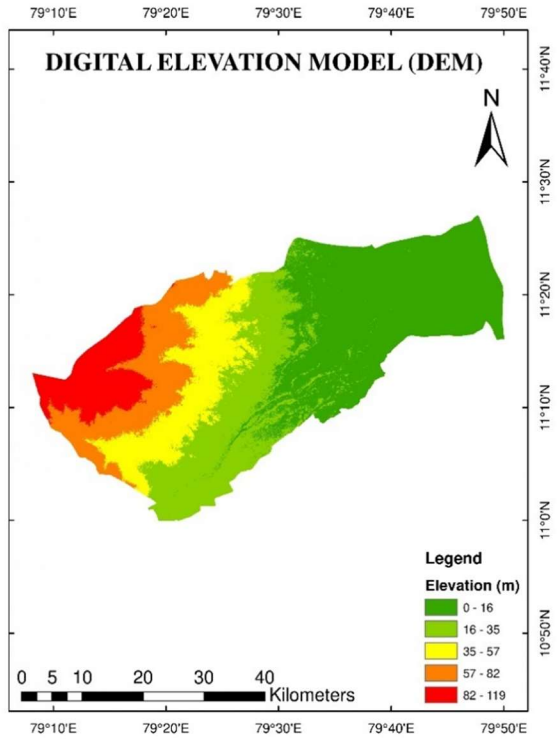

Figure 4 DEM of the Narudaiyar Watershed

Catalyst Research Volume 23, Issue 2, October 2023 Pp. 2226-2244

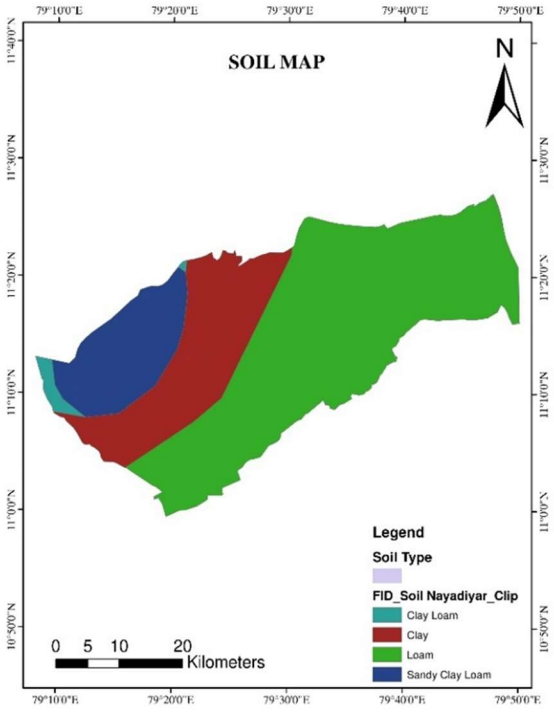

Figure 5 Soil Map of the Narudaiyar Watershed

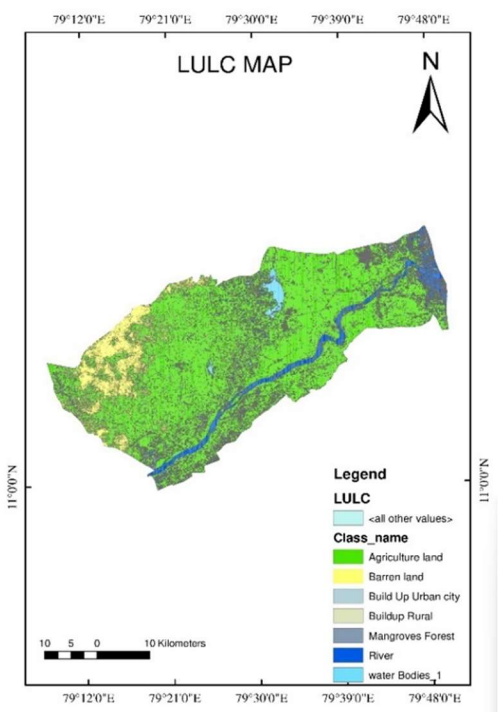

Figure 6 LULC Map of the Narudaiyar Watershed

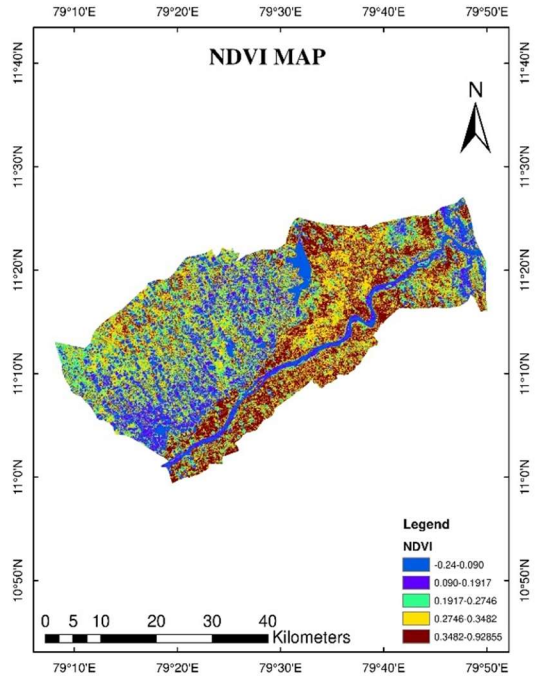

Figure 8 Rainfall Map of the Narudaiyar Watershed

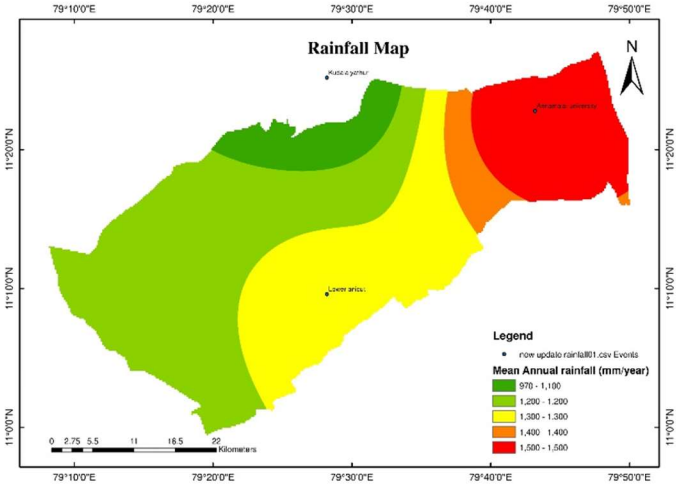

Figure 7 NDVI Map of the Narudaiyar Watershed

Catalyst Research Volume 23, Issue 2, October 2023 Pp. 2226-2244

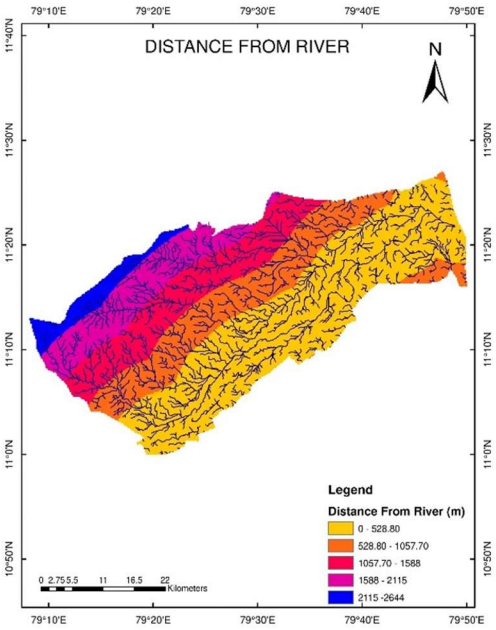

Figure 9 Distance from the River of the Narudaiyar Watershed

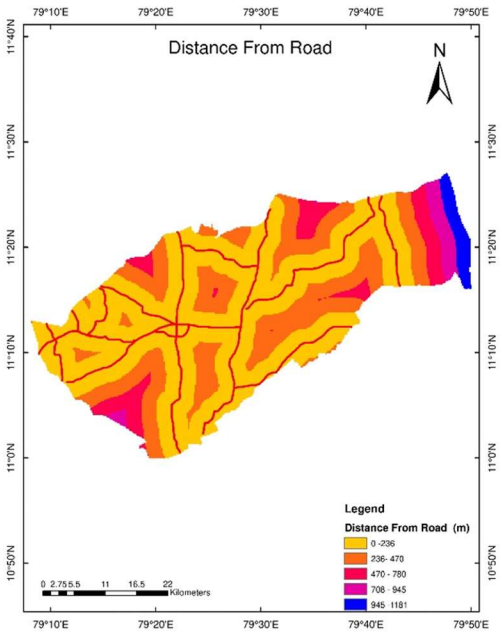

Figure 10 Distance from the Road of the Narudaiyar Watershed

Deluge conducive standard	Units	Section	Frequencies and assessments of exposure categories	Evaluations of Potential Vulnerability
TWI	Level	-7.74 to -3.62	Exceptionally Minor	1
		-3.62 to -1.58	Lower	2
		-1.58 to 0.778	Adequate	3
		0.778 to 4.11	Higher	4
		4.11 to 12.99	Highly significant	5
Elevation	m	0-16	Highly significant	5
		16-35	Higher	4
		35-57	Adequate	3
		57-82	Lower	2
		82-119	Exceptionally Minor	1
Slope	(Degree)^{o}	0-0.656	Highly significant	5
		0.656-1.70	High	4
		1.70-2.88	Moderate	3
		2.88-4.59	Low	2
		4.59-33.46	Exceptionally Minor	1
Precipitation	mm/year	970-1100	Exceptionally Minor	1
		1100-1200	Low	2
		1200-1300	Moderate	3
		1300-1400	High	4
		1400-1500	Highly significant	5
Land use/land cover	Level	Waterbodies & River	Highly significant	5
		Agriculture	Higher	4
		Build Up Rural & Urban	Moderate	3
		Baren land	Lower	2
		Forest	Exceptionally Minor	1
NDVI	Level	-1/54- 0.090	Highly significant	5
		0.090-0.1917	Higher	4
		0.1917-1/5746	Moderate	3
		1/5746-0.3482	Lower	2
		0.3482-0.92855	Exceptionally Minor	1
Proximity to the River	m	0-528	Highly significant	5
		528-1057	High	4
		1057-1588	Moderate	3
		1588-2115	Low	2
		2115-2644	Exceptionally Minor	1
Proximity to the Road	m	0-236	Highly significant	5
		236-470	High	4
		470-780	adequate	3
		780-945	Low	2
		945-1181	Exceptionally Minor	1
Density of outflow	km/km^{2}	<1	Exceptionally Minor	1
		1.17-2.02	Lower	2
		2.02-3.95	Moderate	3
		3.95-4.10	Higher	4
		>6	Highly significant	5

Soil Type	Level	Clay	Highly significant	5
		Sandy Clay Loam	Higher	4
		Clay Loam	Moderate	3
		Loam	Lower	2
		Sand	Exceptionally Minor	1

Table 5 Dimensions of subsidiaries are calculated using (AHP) Comparison matrix.

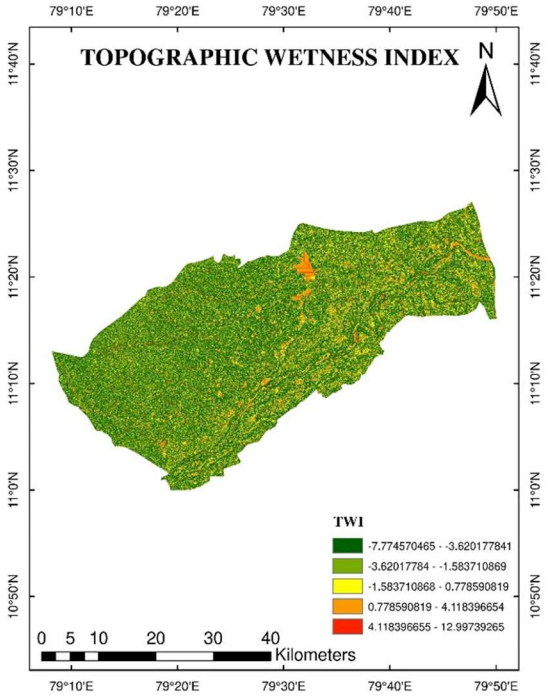

Figure 11 TWI of the Narudaiyar Watershed

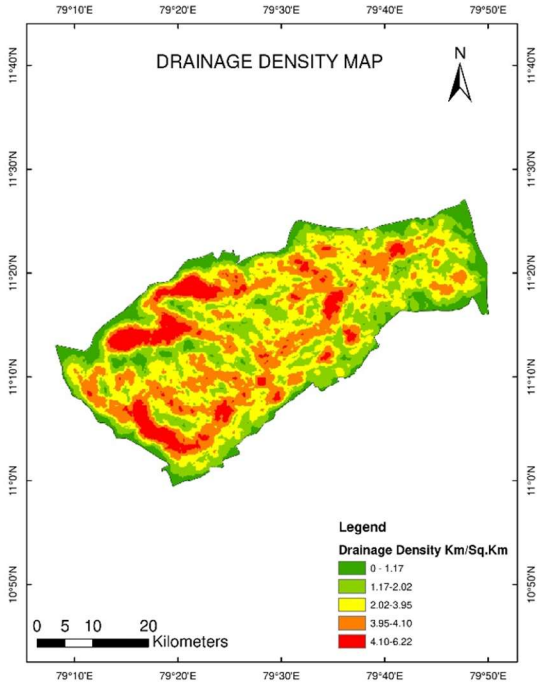

Figure 12 Drainage Density Map of the Narudaiyar Watershed

Catalyst Research Volume 23, Issue 2, October 2023 Pp. 2226-2244

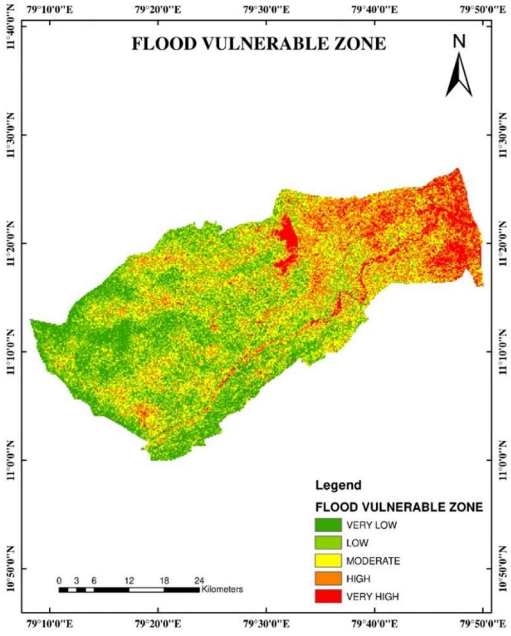

Figure 13 Flood Vulnerable Zone of the Narudaiyar Watershed

Conclusion

The current study identifies flood vulnerability zones as a necessary first step in determining how vulnerable different areas are to natural disasters. The multifaceted decision-making-based AHP model technique was implemented to conduct flood vulnerability research in the Narudaiyar Watershed since it is the most effective and widely used strategy. Because these methods were less expensive and time-consuming, the research employed the analytical hierarchy process (AHP) and GIS approaches. The ArcGIS platform includes a number of integrated variables, including elevation, slope, Rainfall, Land use/Landover, NDVI, TWI, proximity to the river, proximity to road, density of outflow, and kind of soil. A flood-sensitive map has been created as a result, and it shows that 16% of the entire research region levels were extremely high in 37% of cases, moderate in 14% of cases, low in 13% of cases, and exceptionally low in 19% of cases. These regions are typically found along the coastline in the study area's southernmost portion. Additionally, it was discovered that roughly 37% of the entire area of 1884 km2 had a high likelihood of flooding; in order to lower the danger, local and national authorities must pay special attention to these areas. In order to effectively decide on mitigation measures in flood-prone coastal areas, the findings from this study will be an essential tool for those making policies and environmental managers. Using AHP tool tackles could shorten the time taken to discover the suspectable zonal vicinity of a flood while rendering it simple to begin implementing conservation structures in any anticipated zone of a flooded area.

References

1. Bal, PK, Ramachandran, A, Geetha, R, Bhaskaran, B, Thirumurugan, P, Indumathi, J & Jayanthi, N 2015, „Climate change projections for Tamil Nadu deriving high resolution climate

Catalyst Research Volume 23, Issue 2, October 2023 Pp. 2226-2244

data by a downscaling approach using PRECIS",Theoretical and Applied Climatology , https://doi.org/10.1007/s00704-014-1367-9.

2. Bonham-Carter GF (1994) Geographic information systems for geoscientists: modeling with GIS. Pergamon, Elsevier Science Ltd, p 398

3. Botzen WJW, Aerts JCJH, van den Bergh JCJM (2012) Individual preferences for reducing flood risk to near zero through elevation. Mitig Adapt Strateg Glob Change (2):229–244. https://doi.org/10.1007/ s11027-012-9359-5

4. Chakraborty S, Mukhopadhyay S (2019) Assessing flood risk using analytical hierarchy process (AHP) and geographical information system (GIS): application in Coochbehar district of West Bengal, India. Nat Hazards 99(1):247–274

5. Charlton R, Fealy R, Moore S, Sweeney J, Murphy C (2006) Assessing the impact of climate change on water supply and flood hazard in Ireland using statistical downscaling and hydrological modeling techniques. Clim Chang 74:475–491

6. CWC (2018) ,Central water commission annual report 2018-2019. http://cwc.gov.in/sites/defau lt/files /arcwc 2018-19.pdf. Accessed 22 Sep 2020

7. Dandapat K, Panda GK (2017), Flood vulnerability analysis and risk assessment using analytical hierarchy process. Model Earth Syst Environ 3(4):1627–1646

8. Danumah JH, Odai SN, Saley BM, Szarzynski J, Thiel M, Kwaku A et al (2016) Flood risk assessment and mapping in Abidjan district using multi-criteria analysis (AHP) model and geoinformation techniques, (cote d'ivoire). Geoenviron Disasters 3(1):10.

9. Das S, Pardeshi SD (2018) Morphometric analysis of Vaitarna and Ulhas river basins, Maharashtra, India: using geospatial techniques. ApplWater Sci 8(6):158. https://doi.org/10.1007/s13201-018-0801-Z

10. Das S, Pardeshi SD (2018a) Comparative analysis of lineaments extracted from Cartosat, SRTM and Aster DEM: a study based on four watersheds in Konkan region, India. Spat Inf Res 26(1):47–57. https://doi. org/10.1007/s41324-017-0155-x

11. Das S, Pardeshi SD, Kulkarni PP, Doke A (2018) Extraction of lineaments from different azimuth angles using geospatial techniques: a case study of Pravara basin, Maharashtra, India. Arab J Geosci 11: 160. https://doi.org/10.1007/s12517-018-3522-6

12. De Brito MM, Evers M (2016) Multi-criteria decision-making for flood risk management: a survey of the current state of the art. assessment at national scale. J Marine Sci Eng 5(4):51

13. De, US & Dandekar, MM 2001, „Natural Disasters in Urban Areas", The Deccan Geographer, vol. 39, no. 2.

14. De, US, Singh, GP & Rase, DM 2013, „Urban flooding in recent decades in four mega cities of India", J. Ind.

15. Di Risio M, Bruschi A, Lisi I, Pesarino V, Pasquali D (2017) Comparative analysis of coastal flooding vulnerability and hazard

16. DMSG (Disaster Management Support Group) 2001, The Use of Earth Observing Satellites for Hazard Support Group, Report, NOAA, Department of Commerce, USA.

17. Dou X, Song J,Wang L, Tang B,Xu S, Kong F, JiangX (2017) Flood risk assessment and mapping based on a modified multi-parameter flood hazard index model in the Guanzhong Urban Area, China. Stoch Environ Res Risk Assess 32:1131–1146. https://doi.org/10.1007/ s00477-017-1429-5

18. Forte, F & Strobl, R 2006, „A methodology using GIS, aerial photos and remote sensing for loss estimation and flood vulnerability analysis in the Supersano-Ruffano-Nociglia Graben, southern Italy", Environ. Geol., vol. 50, no. 4, pp. 581–594

19. Ghosh S, Carranza EJM, Van-Westen CJ, Jetten VG, Bhattacharya DN (2011) Selecting and weighting spatial predictors for empirical modeling of landslide susceptibility in the Darjeeling Himalayas (India). Geomorphology 131:35–56

20. Gokceoglu C, Sonmez H, Nefeslioglu HA, Duman TY, Can T (2005) The 17 March 2005 Kuzulu landslide (Sivas, Turkey) and landslide susceptibility map of its near vicinity. Eng Geol 81:65–83. https://doi.org/10.1016/j.enggeo.2005.07.011

21. Goswamy, BN, Venugopal, VN, Sengupta, D, Madhusoodanan, MS, & Xavier, PK 2006,„Increasing trend of extreme rain events over India in a warming environment", Science, vol. 314, pp. 1442-1445.

22. Hennessey, KJ, Gregory, JM & Mitchell, JFB 1997, „Changes in daily precipitation under enhanced greenhouse conditions", Climate Dynamics, vol. 13, pp. 667–680. https

23. ://doi.org/10.1186/s4067 7-016-0044-y

24. IPCC (Intergovernmental Panel on Climate Change) (2007), Climate Change 2007: The physical science basis. Contribution of working group I to the fourth assessment report of the intergovernmental panel on climate change, edited by Solomon, S et al., Cambridge Univ. Press.

25. Jeb, DN & Aggarwal, SP 2008, „Flood Inundation Hazard Modeling of the River Kaduna Using Remote Sensing and Geographic Information Systems", Journal of Applied Sciences Research, vol. 4, pp. 1822-1833.

26. Kaur H, Gupta S, Prakash S, Thapa R, Mandal R (2017) Geospatial modelling of flood susceptibility pattern in a subtropical area of Khole, M & De, US 2001, ‚Socio-economic impacts of natural disasters", WMO. Bulletin, vol. 50, pp. 35–40.

27. Khosravi K, Pourghasemi HR, Chapi K, Bahri M (2016b) Flash flood susceptibility analysis and its mapping using different bivariate models in Iran: a comparison between Shannon's entropy, statistical index, and weighting factor models. EnvironMonit Assess 188:

28. Lawal DU, Matori AN, Hashim AM,Wan Yusof K, Chandio IA (2012) Detecting flood susceptible areas using GIS-based analytic hierarchy process. Int Proc Chem Biol Environ Engg 28:1–5

29. Lim J, Lee K (2017) Investigating flood susceptible areas in inaccessible regions using remote sensing and geographic information system. Environ Monit Assess 189:96

30. Masoudian, M., 2009. The topographical impact on effectiveness of flood protection measures (Ph.D. thesis).Faculty of Civil Engineering, Kassel University, Germany. URL<http://www.uni-kassel.de/upress/online/frei/978-3-89958-790-6.volltext.frei. pdf>. Visited on 2013-12-10.

Catalyst Research Volume 23, Issue 2, October 2023 Pp. 2226-2244

31. Mojaddadi H, Pradhan B, Nampak H, Ahmad N, Ghazali AHB (2017) Ensemble machine-learning-based geospatial approach for flood risk assessment using multi-sensor remote- sensing data and GIS. Geomatics Nat Hazard Risk 8:1080–1102

32. Mundhe N (2019). Multi-criteria decision making for vulnerability mapping of flood hazard: a case study of Pune city. J GeographStud 2(1):41–52. https ://doi.org/11/51523 /gcj5.18020 105Nat Hazards Earth Syst Sci 16(4):1019–1033NOAA Coastal services centre1998 Glossary of Coastal Terminology, Publication No. 98– 11/2.

33. Pradhan B (2009), Groundwater potential zonation for basaltic watersheds using satellite remote sensing data andGIS techniques. Open Geosci 1:120–129. https://doi.org/11/5478/v10085-009-0008-5

34. Risi RD, Jalayer F, Paola FD, Lindley S (2017) Delineation of flooding risk hotspot based on digital elevation model, calculated and historical flooding extents: the case of Ouagadougou. Stoch Environ Res Risk Assess. 32:1545–1559. https://doi.org/10.1007/s 004 77-017-1450-8

35. Rocha C, Antunes C, Catita C (2020) Coastal vulnerability assessment due to sea level rise: the case study of the Atlantic Coast of Mainland Portugal. Water 12(2):360

36. Rojas R, Feyen L, Bianchi A, Dosio A (2012), Assessment of future flood hazard in Europe using a large ensemble of bias-corrected regional climate simulations. J Geophys Res Atmos 117:D17109. https://doi. org/10.1029/2012JD017461

37. Roy DC, Blaschke T (2015) Spatial vulnerability assessment of floods in the coastal regions of Bangladesh. Geomatics Nat Hazards Risk 6(1):21–44

38. Saaty, TL 1980, „The Analytic Hierarchy Process: Planning, Priority Setting“, Resource Allocation, Mcgraw-Hill, New York, NY.

39. Sampson CC, SmithAM, Bates PD, Neal JC,Alfieri L, Freer JE (2015) A high-resolution global flood hazard model. Water Resour Res 51:7358–7381

40. Senanayake IP, Dissanayake DMDOK, Mayadunna BB, Weerasekera WL (2016) An appro - ach to delineate groundwater recharge potential sites in Ambalantota, Sri Lanka using GIS techniques. Geosci Fron 7:115–124

41. Sulaiman NA, Mastor TA, Mat MSC, Samad AM (2015), Flood hazard zoning and risk assessment for Bandar Segamat sustainability using analytical hierarchy process (AHP). In: 2015 IEEE 11th international colloquium on signal processing and its applications(CSPA), pp 72–77. IEEE

42. Szynkowska, M 2015, „Flood in Tamil Nadu, India disaster induced displacement“, Retrieved from:http://labos.ulg.ac.be/hugo/wp-content/uploads/sites/38/2017/11/The-State-ofEnvironmental-Migration-2016-152-172.pdf. Accessed 02 Oct 2017.West Bengal, India. Environ Earth Sci 76:339

43. Yule GU (1912) On the methods of measuring association between two attributes. J R Stat Soc 75:579–642